Journal of Physiology (1990), **423**, *pp.* 137–153
With 9 figures
Printed in Great Britain

THE MEMBRANE PROPERTIES AND FIRING CHARACTERISTICS OF RAT JAW-ELEVATOR MOTONEURONES

BY JANE MOORE AND KWABENA APPENTENG
From the Department of Physiology, University of Leeds, Leeds LS2 9NQ

(*Received 6 July 1989*)

SUMMARY

1. We have determined the membrane and firing properties of fifty-six jaw-elevator motoneurones in rats that were anaesthetized with pentobarbitone, paralysed and artificially ventilated.

2. Forty-two neurones were identified as masseter motoneurones and fourteen as masseter synergist motoneurones. The membrane potentials for the sample ranged from −60 to −86 (mean = −68; S.D. = 7·3; $n = 56$), and spike amplitudes from 50 to 95 mV. The duration of the after-hyperpolarization following antidromic spikes in masseter motoneurones ranged from 15 to 50 ms (mean = 30; S.D. = 12·8) and their amplitudes from 1·0 to 4·5 mV (mean = 2·7; S.D. = 2·2; $n = 42$).

3. The mean input resistance for the total sample was 2·3 MΩ (S.D. = 0·9; $n = 56$), membrane time constant 3·9 ms (S.D. = 0·9; $n = 48$) and rheobase 4·2 nA (S.D. = 2·6; $n = 56$). The distribution of these parameters was independent of membrane potential. We found no significant interrelationships between the membrane properties and one interpretation of this is that our sample may be drawn from a homogenous population of motoneurones. We also suggest that elevator motoneurones may have a lower R_m (specific membrane resistivity) value than cat hindlimb motoneurones because they have a similar range of input resistance values but only half the total surface area.

4. Forty-six out of forty-nine neurones fired repetitively to a depolarizing current pulse at a mean threshold of 1·6 × rheobase. Current–frequency plots were constructed for thirteen neurones and all but one showed a primary and secondary range in the firing of the first interspike interval. The mean slope in the primary range was 31 impulses s^{-1} nA^{-1} and 77 impulses s^{-1} nA^{-1} for the secondary range. The mean minimal firing frequency for steady firing was 26 impulses s^{-1} and, in response to an increase of stimulation, the rate increased monotonically with a slope of 11 impulses s^{-1} nA^{-1}.

5. The dynamic sensitivity of twelve neurones was assessed from their response to ramp waveforms of current of constant amplitude but varying frequencies (0·2–2 Hz). Firing initially increased along a steep slope up to a frequency of between 40 and 60 impulses s^{-1} and then increased along a much shallower slope. Both the threshold for eliciting firing and the firing at the transition point of the two slopes remained constant with changes in ramp frequency. This suggests that within the frequency range studied firing is dependent primarily on the amplitude of injected current and not on its rate of change.

INTRODUCTION

Our underlying aim is to assess the integrative properties of jaw-elevator motoneurones and an important step towards this goal consists of obtaining a description of the population membrane and firing properties. However, the only published data of relevance consists of one report of the firing characteristics of two elevator motoneurones (cat: Takata, Fujita & Kanamori, 1982), two studies of input resistance (rat: Mikhailov & Kuneev, 1981; Vornov & Sutin, 1986) and one of rheobase (rat: Mikhailov & Kuneev, 1981). Membrane time constant values have not been determined, nor have both membrane and firing properties been determined for the same sample of elevator motoneurones. Therefore much of the essential information needed for an assessment of the integrative properties of these neurones is lacking.

There is in contrast a large body of information on the electrical properties of motoneurones in the cat lumbosacral cord (Granit, Kernell & Shortess, 1986*3a*; Burke & ten Bruggencate, 1971; Kernell, 1965*a*, *b*, 1983; Gustafsson & Pinter, 1984*a*, *b*; Zengel, Reid, Sypert & Munson, 1985). Systematic studies of the properties of other groups of motoneurones have been relatively rare (abducens: Grantyn & Grantyn, 1978; phrenic: Jodkowski, Viana, Dick & Berger, 1987, 1988; neck and shoulder; Rose & Vanner, 1988) and so it has been difficult to ascertain the general significance of particular features of organization described for lumbosacral motoneurones. Therefore the aims of this study were first to determine the electrical properties of a population of elevator motoneurones and then to compare these to those of hindlimb motoneurones. Preliminary abstracts of this work have been published (Appenteng & Moore, 1986, 1987).

METHODS

Surgical preparation. This was essentially as described earlier by Appenteng, Conyers & Moore (1989). In brief, nine rats in the weight range 200–250 g were initially anaesthetized with a mixture of halothane in oxygen. A femoral venous catheter was inserted and further anaesthesia maintained by I.V. infusions of pentobarbitone (initial dose = 60 mg kg^{-1}). The trachea was cannulated and blood pressure monitored by a cannula in the femoral artery. The left masseter nerve was exposed in continuity and a pair of silver wires placed around the nerve to allow electrical stimulation. Animals were then transferred to a stereotaxic holder and a hole drilled in the cranium to allow insertion of glass microelectrodes at the co-ordinates of the V motor nucleus. Animals were paralysed with gallamine triethiodide and artificially ventilated for the duration of the experiment. A bilateral pneumothorax was performed and end-tidal carbon dioxide levels monitored. The animals were maintained deeply anaesthetized throughout all stages of the experiment. The criterion used was that a noxious paw-pinch should elicit no change in blood pressure and under these conditions there was no flexion withdrawal reflex in the unparalysed animal.

Electrodes. These were pulled from thin-walled glass (o.d. = 1·2 mm, i.d. = 0·94 mm) and filled with a 3 M-KCl solution. Their initial tip resistances varied from 15 to 20 MΩ and they were then bevelled down ideally to resistances of between 5 and 10 MΩ. Electrodes were only accepted for use if they could pass at least 20 nA of current in both the hyperpolarizing and depolarizing directions without rectification as we had established in pilot experiments that such electrodes were capable of repeated penetrations through 8 mm of brain without blocking or breaking (signalled by a change in the tip resistance) and yet be sharp enough to penetrate motoneurones whose mean soma diameter is 25 μm (Moore & Appenteng, 1989). Electrode tips were routinely dipped in dimethyldichlorosilane immediately before use.

Recording. This was by means of a Neurolog DC preamplifier (NL102G) equipped with active bridge balance and negative capacitance compensation. The bridge output of the amplifier and a signal proportional to the current injected were recorded on an FM tape-recorder (Racal Store 7; bandwidth, 0–5 kHz). Also recorded on tape were the pulses triggering the nerve stimulator and the stimulus pulse initiating current injection down the microelectrode.

Protocol. Our experimental protocol was to first identify the masseter motoneurone pool within the V motor nucleus. This was on the basis of the amplitude of the antidromic field potential recorded in response to electrical stimulation of the masseter nerve. The latency of this field was some 0·5 ms and its amplitude ranged from 1·5 to 2 mV when the electrode was optimally situated within the motoneurone pool. Current pulses were passed down the electrode and the bridge circuit adjusted so that the voltage trace was continuous at the make-and-break artifacts. Penetrations were then made into neurones that were identified as masseter or masseter synergist motoneurones on the basis of the criteria described by Appenteng, Donga & Williams (1985). Following penetration cells were left to stabilize for some 5 min before their membrane properties were determined. Neurones were only accepted for inclusion in this study if they had membrane potentials of at least −60 mV 5 min after penetration.

The neuronal input resistance (R_n) was determined from the transmembrane voltage response to a 2 nA, 50 ms hyperpolarizing current pulse (Fig. 1*A*) and membrane time constant (τ_0) from the response to either a 50 or 10 ms pulse applied at an intensity of 1 nA or less. We carefully examined the output of the bridge balance amplifier on a fast sweep speed (both during the recording and on subsequent playback of the tape) specifically to assess if there had been an alteration of the electrode resistance following penetration. This was assumed to have remained constant if following the initial capacitative transient the slower membrane response took off smoothly from the baseline membrane potential. We did not attempt to change the bridge balance point once intracellular and rejected data from neurones in which the membrane response was preceded by an abrupt step following the capacitative transient as this indicated that the electrode resistance had altered following penetration. The masseter nerve was stimulated after each cycle of current injection in order to check that the spike amplitude had not deteriorated. The membrane potential was also continuously monitored and data were not accepted from units in which the resting membrane potential changed by more than 5 mV while the membrane properties were being determined. Typically the intracellular and extracellular response to between 8 and 32 cycles of current injection were recorded on tape. They were subsequently digitized at a frequency of 80 kHz using a C.E.D. 1401 interface (Cambridge Electronic Design), averaged and the transmembrane voltage response calculated. R_n was calculated from the peak transmembrane voltage response to the current injected. The membrane time constant τ_0 was calculated from a plot of the natural log of 'decay' of the potential with time (Fig. 1*B*). To do this the maximum voltage response to the current pulse was first determined, subtracted from each voltage value and the natural log of the resultant plotted against time. We ignored all voltage changes occurring during the first millisecond of the current pulse. The linear portion of each plot was determined by eye and the best-fit straight line to the intervening data points calculated by the method of least squares. The value of τ_0 was then given by the time for the voltage to decay to 1/e of its initial value. Among the assumptions made in the derivation of τ_0 are that the membrane behaves passively, R_m (specific membrane resistivity) is constant throughout the neurone and that the dendritic tree can be approximated electrically as equivalent to a single cylinder (Rall, 1959, 1977). The latter two assumptions have recently been questioned (Bras, Gogan & Tyc-Dumont, 1987; Appenteng & Moore, 1988; Fleshman, Segev & Burke, 1988; Moore, 1988; Rose & Vanner, 1988; Clements & Redman, 1989) but the magnitude of the error cannot be assessed until a quantitative description of the electrical geometry of the neurones in question has been obtained. Therefore the caveat made is that the values of τ_0 presented here for elevator motoneurones may need to be corrected at some stage in the future.

Rheobase was routinely determined from the response to a 50 ms depolarizing current pulse. The current intensity was then slowly increased so as to obtain sustained firing from neurones (Fig. 1*C* and *D*). In some neurones firing in response to different waveforms of injected current (i.e. ramp-and-hold, ramp, saw-tooth and sinusoidal) was also studied. Recording sites were routinely verified as being in the motor nucleus by reconstruction of electrode tracks.

RESULTS

Unit identification and spike properties

The data for this study are drawn from fifty-six elevator motoneurones whose membrane potentials (V_m) ranged from −60 to −86 mV (mean = −68; S.D. = 7·3:

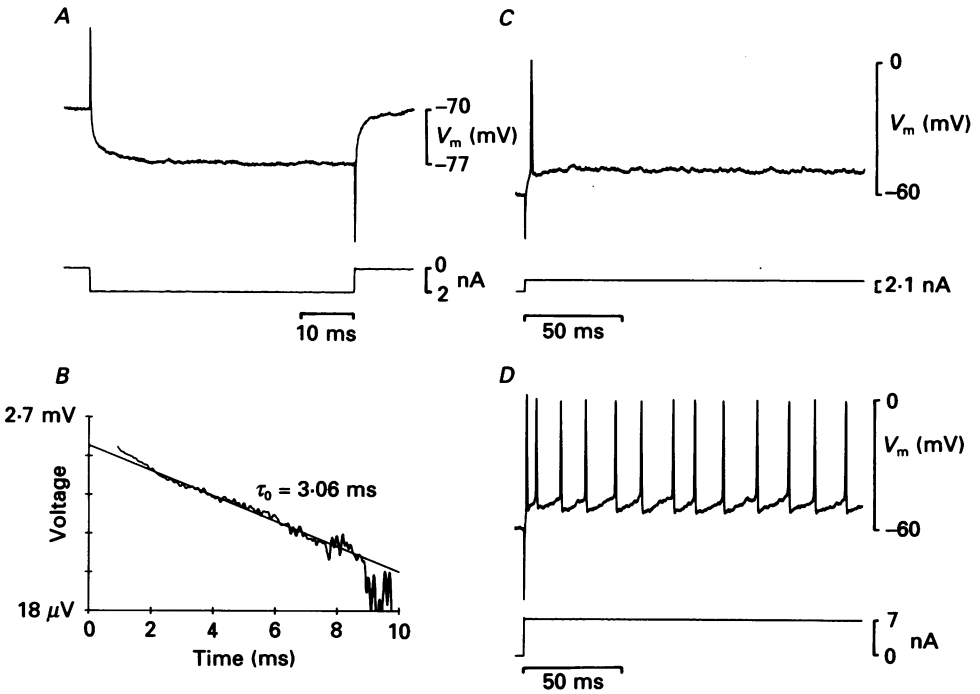

Fig. 1. Steps in the determination of input resistance (*A*) and membrane time constant (*B*) of a masseter motoneurone. *A* shows a single sweep of the intracellular response of the neurone to a 50 ms, 2 nA hyperpolarizing current pulse. *B* shows a semilogarithmic plot of the averaged (32 sweeps) transmembrane voltage response to a 1 nA hyperpolarizing current pulse. The continuous line in *B* is the best-fit straight line to the linear portion of the plot; note that the first millisecond of the data obtained after the onset of the current pulse is ignored in the semilogarithmic plot. *C* shows the determination of rheobase for a neurone in response to a 500 ms current pulse; *D* shows the repetitive firing of the same neurone to a 500 ms current pulse. Top trace in *A*, *C* and *D* shows membrane potential and bottom trace the current. Traces in *A*, *C* and *D* filtered between DC and 5 kHz and digitized at 40 kHz in *A* and 80 kHz in *C* and *D*.

Fig. 2*A*). Forty-two were antidromically activated at latencies of 0·42–0·65 ms (mean = 0·55; S.D. = 0·27) following electrical stimulation of the masseter nerve and so were identified as masseter motoneurones. We calculated their conduction velocities by assuming a conduction distance of 15 mm and a utilization time of 0·1 ms (Moore & Appenteng, 1989). The values calculated ranged from 27 to 47 m s^{-1} (mean = 34; S.D. = 5·0) and compare with a range of 16–39 m s^{-1} derived from estimates of the fibre diameters of rat elevator motoneurones labelled by intracellular injection of horseradish peroxidase (Moore & Appenteng, 1989). The recordings were all judged to be from an intrasomatic site because of the presence of an inflexion on the rising

phase of the spike (Brock, Coombs & Eccles, 1952). This was most simply revealed by applying two closely spaced stimuli at the critical interval for the soma–dendritic spike (Fig. 2*C*), a value invariably less than 4 ms. The remaining fourteen neurones in our sample showed a monosynaptic EPSP but no antidromic spike and so were

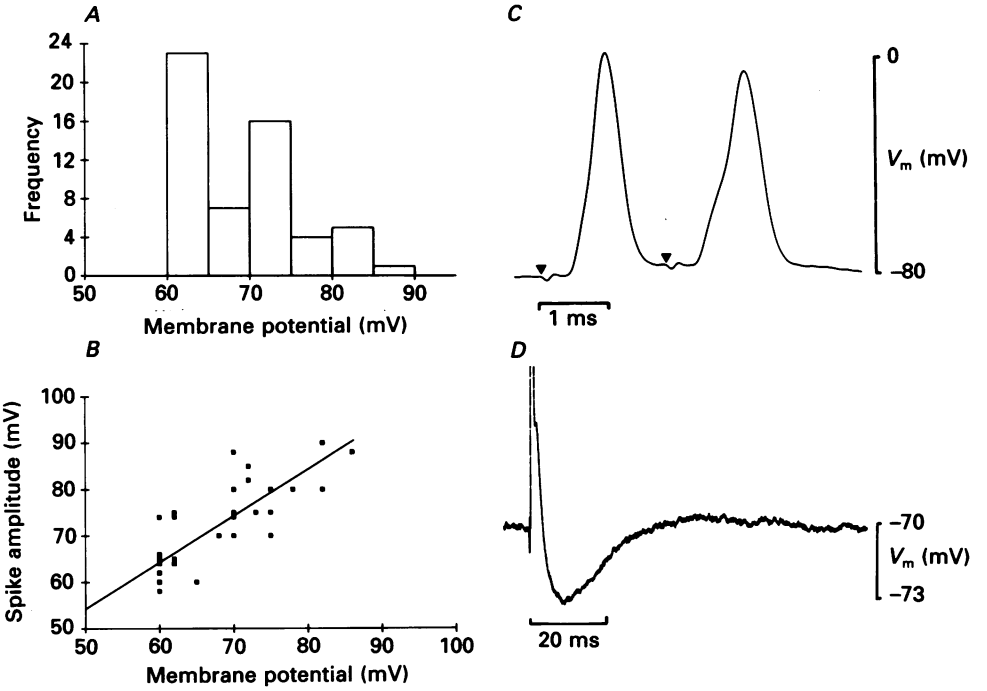

Fig. 2 *A*: distribution of membrane potentials for the total sample of masseter and masseter synergist motoneurones. *B*: plot of antidromic spike amplitudes against membrane potential for masseter motoneurones. Continuous line is the best-fit straight line to data and has a slope of 1·0. *C*: response of a masseter motoneurone to two closely spaced (separation of 1·8 ms) electrical stimuli applied to the masseter nerve. Arrowheads mark onset of stimulus pulses. Both stimuli elicit antidromic spikes at a latency of 0·41 ms but note the more pronounced inflexion on the rising phase of the second spike. *D*: delayed depolarization and after-hyperpolarization following an antidromic spike in a masseter motoneurone (4 sweeps averaged). Start of time bar in *D* marks onset of masseter nerve stimulation.

assumed to be masseter synergist motoneurones for the reasons outlined by Appenteng *et al.* (1985). The EPSP latencies in these ranged from 1·0 to 3·1 ms (mean = 1·6; S.D. = 1·2) and the amplitudes from 1·0 to 5·0 mV (mean = 1·9; S.D. = 1·4). The synaptically evoked spikes ranged from 50 to 95 mV in amplitude and the membrane potentials of the neurones from −60 to −80 mV. There was no difference in the membrane potentials of masseter and masseter synergist motoneurones ($P > 0·05$).

The antidromic spikes in masseter motoneurones ranged from 58 to 90 mV in amplitude (mean = 71·0; S.D. = 8·9; $n = 42$: Fig. 2*B*) and seventeen of them were accompanied by particularly pronounced delayed depolarizations (Granit, Kernell & Smith, 1963*b*) which were seen as transient reversals on the falling phase of the spikes

(Fig. 2*D*). The amplitude of these delayed depolarizations ranged from 2·0 to 8·0 mV (mean = 5·7; S.D. = 4·7) above the initial resting membrane potential and their durations (measured from the peak of the delayed depolarization to the point where the potential returned to the resting value) from 1·0 to 4·5 ms (men = 2·7; S.D. = 2·2).

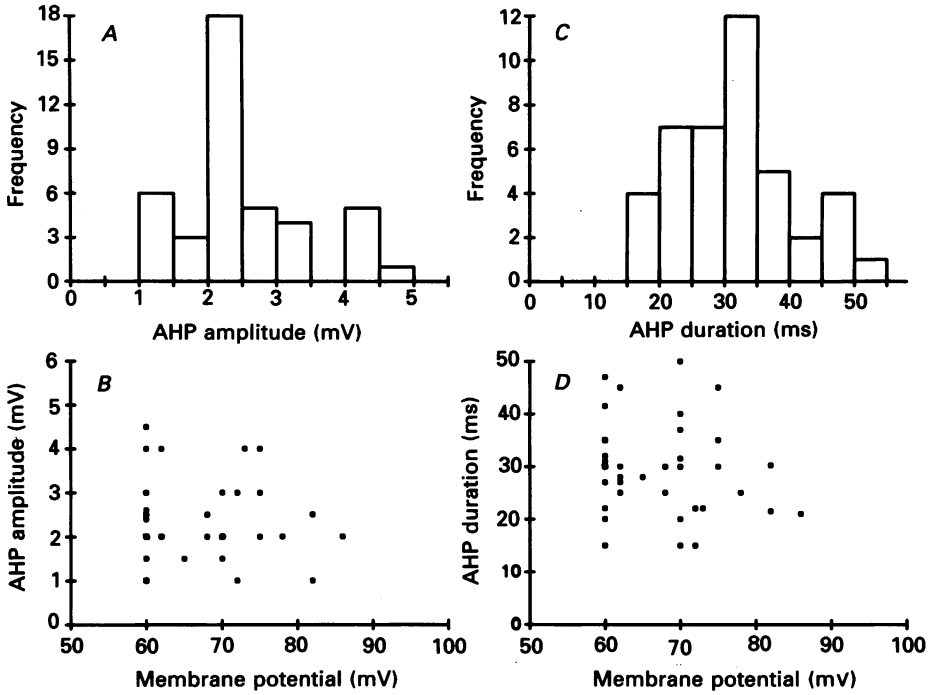

Fig. 3. Distribution of the amplitude (*A*) and duration (*C*) of the AHPs following antidromic activation of masseter motoneurones. The plots in *B* and *D* show that these parameters vary independently of membrane potential.

The delayed depolarization was followed by an after-hyperpolarization (AHP) which reached a peak amplitude 6–11 ms after the onset of the antidromic spike (Fig. 2*D*). The mean amplitude of the AHPs was 2·3 mV (range = 1·0 to 4·5; S.D. = 0·8; $n = 42$: Fig. 3*A*) and their duration (measured from the onset of the spike to the point where the potential returned to the resting value) was 30 ms (range = 15·0 to 50; S.D. = 12·8: Fig. 3*C*). Both these parameters were independent of V_m (Fig. 3*B* and *D*) and also of each other.

Membrane properties

Our initial step was to identify the linear region of the current–voltage relationship of elevator motoneurones and the procedure adopted is illustrated for one neurone in Fig. 4*A*. Increases in the current injected result in an increase in the magnitude of the membrane potential change seen and also an alteration in the form of this change. For example, injection of a 1 nA hyperpolarizing current elicits a membrane potential change that reaches a peak within 5 ms and then remains constant throughout the remaining period of current injection. A 2 nA current elicits a

potential change that shows a slight decrease in magnitude after the peak (i.e. sag; Ito & Oshima, 1965). Injection of a 4 nA hyperpolarizing current results in a more pronounced sag of the voltage response (Fig. 4*A*). We quantified the magnitude of sag by determining the percentage reduction in voltage from the peak value to the

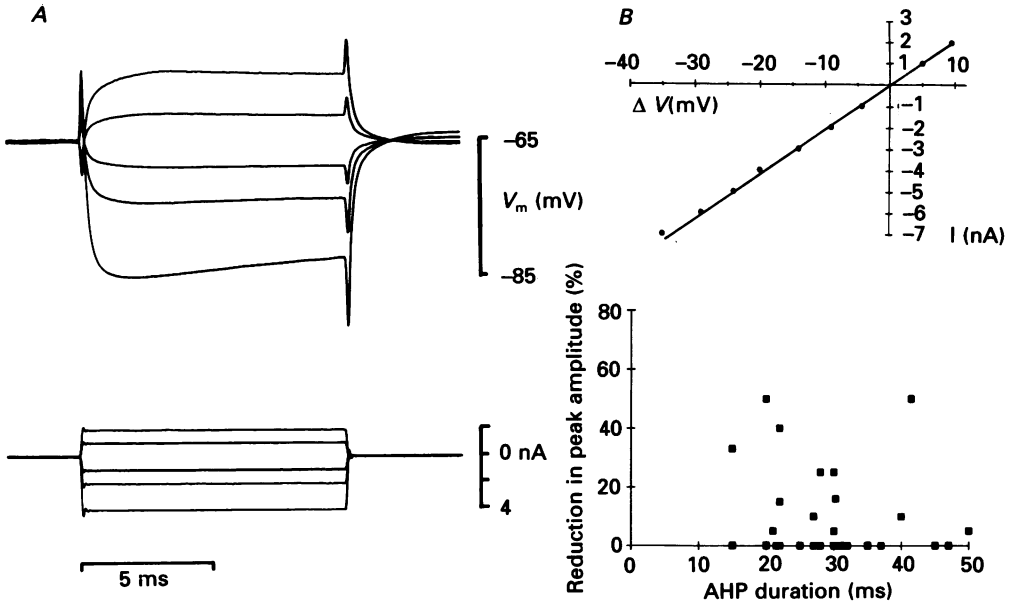

Fig. 4. *A*: qualitative changes in the response of a masseter motoneurone to current injections. Top traces show superimposed membrane potential changes (each the average of 10 sweeps) in response to injection of different amplitudes of depolarizing and hyperpolarizing currents. The bottom trace shows the applied currents; the intensities used were 1 and 2 nA in the depolarizing direction; 1, 2 and 4 nA in the hyperpolarizing direction. Note the pronounced sag in response to injection of 4 nA hyperpolarizing current. *B*: plot of the peak transmembrane voltage response against injected current for the neurone seen in *A*. *C*: plot of magnitude of sag in response to a 2 nA, 50 ms current injection against the duration of the AHP of the neurone.

steady value in response to a standard 2 nA, 50 ms current pulse. Eighteen of the fifty-six motoneurones showed sag under these conditions and the magnitude of this ranged from 5 to 67%. Gustafsson & Pinter (Fig. 13, 1984*a*) have reported values up to approximately 45% (equivalent to a ratio of 0·55 for the steady/peak voltage) for a sample of lumbosacral motoneurones. They noted a tendency for sag to be more developed in cells with short AHP durations than in those with longer AHPs. For the units which showed sag in our sample there appeared to be some tendency for its magnitude to be greater in cells with shorter AHP durations (Fig. 4*C*) but this was not statistically significant.

The peak voltage deflection in response to a hyperpolarizing current pulse, or a depolarizing one at an intensity below rheobase, was linearly related to the amplitude of injected current over a wide range and was apparently unaffected by the presence or absence of sag (Fig. 4*B*). We obtained current–voltage relationships for a sample of five cells and in each case obtained a linear relationship over the range tested (25–38 mV from resting membrane potential). We therefore routinely

determined R_n from the voltage deflection at a single current intensity. Sag would be expected to result in an underestimation of membrane time constants and so to guard against this we did not calculate τ_0 values for responses where sag was evident.

Figure 5 shows the distribution of values of R_n (Fig. 5*A*), τ_0 (Fig. 5*C*) and rheobase

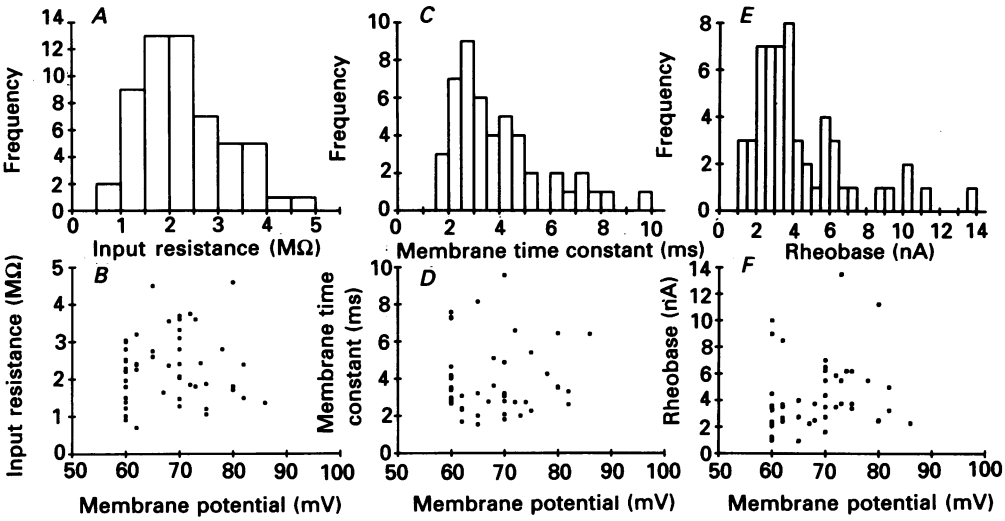

Fig. 5. Frequency distribution of input resistance (*A*), time constant (*C*) and rheobase (*E*) for the total sample of neurones. The scatter plots in *B*, *D* and *F* show variation of these parameters with membrane potential. Only rheobase appears to vary systematically with membrane potential although the relationship is not statistically significant.

(Fig. 5*E*) for the total sample of neurones. There were no significant differences in the values obtained for masseter and masseter synergist motoneurones ($P > 0{\cdot}05$ in all cases). Values of R_n ranged from 0·7 to 4·6 MΩ (mean = 2·3; S.D. = 0·9; $n = 56$), τ_0 from 1·5 to 9·6 ms (mean = 3·9; S.D. = 0·9; $n = 48$) and rheobase from 0·95 to 13·5 nA (mean = 4·2; S.D. = 2·6; $n = 56$). The distributions of R_n, τ_0 and rheobase values were independent of membrane potential (Fig. 5*B*, *D* and *F*).

We have tested for inter-relations between the passive properties, rheobase and AHP duration of our neurones as systematic variations in these properties have been reported for different functional subtypes of hindlimb motoneurones (Gustafsson & Pinter, 1984*a*, *b*; Zengel *et al.* 1985). Specifically, significant relationships have been reported between τ_0 and R_n, the inverse to τ_0 and rheobase, input conductance and rheobase, and AHP duration and rheobase (Gustafsson & Pinter, 1984*a*, *b*). Figure 6 shows plots of these parameters for our data and in each case it is evident that there is no relationship between the two variables. Therefore there is either no systematic variation in membrane properties among elevator motoneurones or alternatively our sample is drawn predominantly from a single functional subtype of motoneurone.

Firing characteristics

Forty-six out of forty-nine neurones tested fired repetitively to a 50 ms depolarizing current pulse when this was increased to intensities of between 1·0 and 4·2× (mean = 1·6×) rheobase. The three neurones which did not fire repetitively

appeared perfectly healthy in that they had membrane potentials of −65 to −73 mV and spike amplitudes of 70–75 mV.

We were able to examine systematically the relationship between firing rate and injected current for thirteen cells and for this we used currents of duration 500 ms.

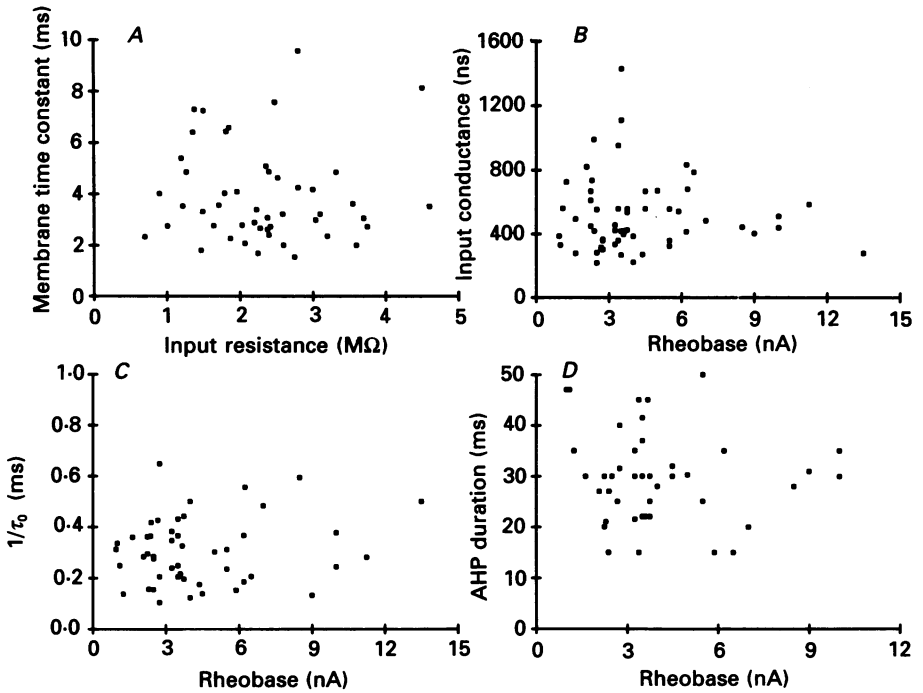

Fig. 6. Plots of the relationship between membrane time constant and input resistance (*A*; $n = 48$), input conductance and rheobase (*B*; $n = 56$), the inverse of the membrane time constant and rheobase (*C*; $n = 48$), and AHP duration and rheobase (*D*; $n = 42$). None of the relationships is significant.

Figure 7 shows plots of firing during the first interspike interval and the steady firing rate for four neurones. In each case both a primary and secondary range can be seen in the firing during the first interspike interval and in fact only one of the thirteen neurones examined failed to show this pattern. Two neurones (Fig. 7*B* and *C*) showed signs of a tertiary range in firing at high discharge rates. The minimal firing frequency in the primary range varied from 33 to 98 impulses s^{-1} (mean = 54) and the maximum frequency from 88 to 198 impulses s^{-1} (mean = 148). The highest frequencies reached in the secondary range varied from 240 to 450 impulses s^{-1}. The slope of the relationship between firing rate and injected current in the primary range varied from 24 to 49 impulses s^{-1} (mean = 31) and from 45 to 119 impulses s^{-1} nA^{-1} (mean = 77) in the secondary range. The minimal frequency of steady firing ranged from 8 to 68 impulses s^{-1} (mean = 26) and, in response to an increase of stimulation, the rate increased monotonically with injected current with a slope of 8 to 20 impulses $s^{-1}nA^{-1}$ (mean = 11) up to frequencies of 100 impulses s^{-1}. We did not see a secondary range to the steady firing but this may have been because we never

drove the firing to rates above the maximum primary range firing for the first interspike interval (Kernell, 1965*a*, 1979).

Six of the thirteen neurones whose firing was studied were masseter motoneurones and for these a consistent finding was that the minimal steady firing rate invariably

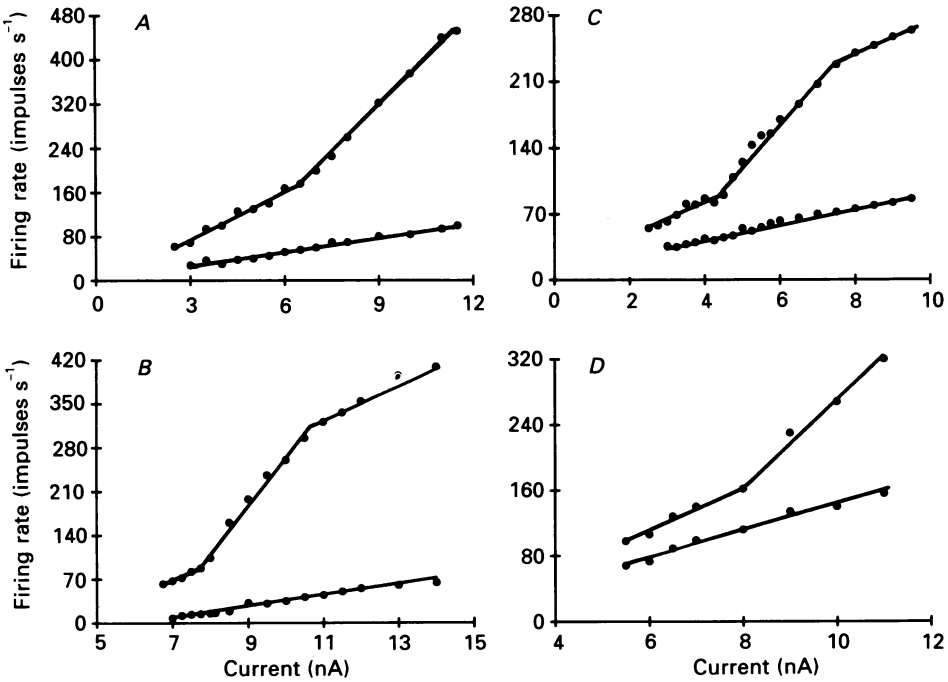

Fig. 7. Relationship between firing rate and injected current for two masseter (*A* and *C*) and two masseter synergist motoneurones (*B* and *D*). In each case the upper trace shows the relationship of the first interspike interval and injected current and the lower one the relationship between steady firing rate and injected current. Note that all four cells show both a primary and secondary range in the plots of their first interspike intervals and in addition that two cells (*B* and *C*) show a tertiary range. Neurone in *A* is the same as that previously shown in Fig. 1*C* and *D*.

occurred at frequencies lower than would be expected on the basis of the reciprocal of the AHP duration (Kernell, 1965*b*, 1983). However Kernell (1965*b*) measured AHP duration to the peak of the positive after-potential whereas we measured it to the point where the potential returned to the baseline because we could not reliably discern the peak of the positive after-potential in our records (e.g. see Fig. 2*D*). Perhaps not unexpectedly then a consistent finding in our data was that steady firing invariably occurred at lower minimal rates than would be expected on the basis of the AHP duration of the neurones. For example the neurones in Fig. 7*A* and *B* were both masseter motoneurones with AHP durations of 27 (Fig. 7*A*) and 21 ms (Fig. 7*C*) and minimal steady firing rates of 28 and 35 impulses s^{-1} respectively as opposed to expected rates of 37 and 48 impulses s^{-1}. However, the difference between the expected and actual rates are sufficiently small as to suggest that AHP duration may be an important factor controlling the firing of elevator motoneurones.

The dynamic behaviour of neurones cannot be adequately assessed by use of step increases in current intensity and so in order to investigate this we used linearly rising ramp waveforms of current. The strategy adopted was to keep the amplitude of the waveform constant for each unit but vary the repetition frequency of the

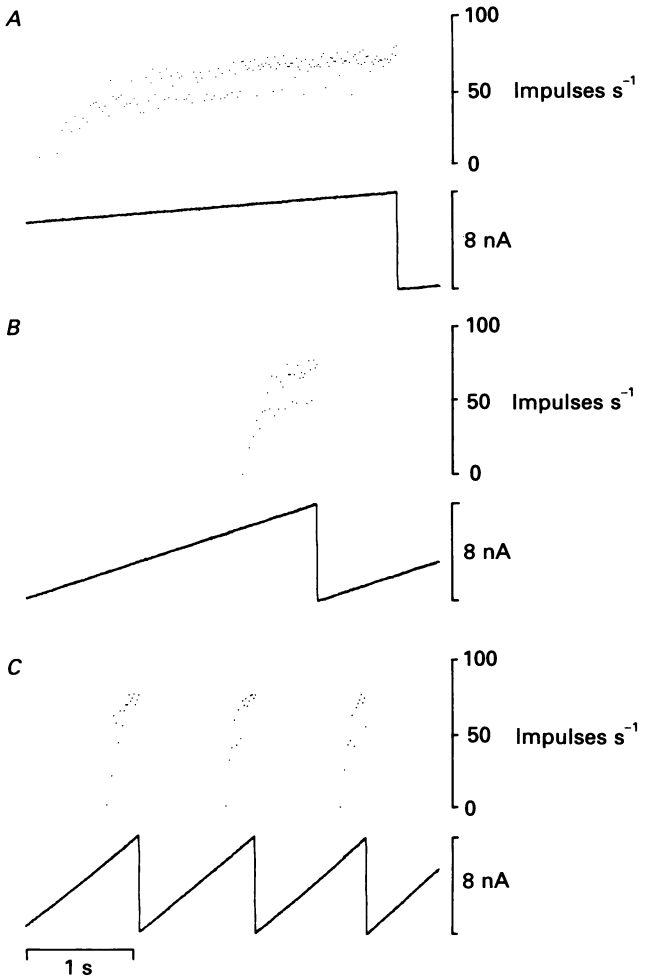

Fig. 8. Motoneurone firing to injection of ramp waveforms of depolarizing current applied at three different velocities (*A*, *B* and *C*). Top trace in each panel shows instantaneous firing frequency of the neurone and lower trace the injected current. Note that in each case firing initially increases smoothly up to a rate of about 50 impulses s^{-1} after which it continues to increase along a much shallower slope. Data from same neurone as shown in Fig. 7*D*.

ramps from 0·2 to 2 Hz. The final amplitude of the ramps was adjusted to elicit an instantaneous firing rate of between 80 to 100 impulses s^{-1} as this would correspond to firing near the top end of the steady firing rate described above. Figure 8 shows the characteristic firing shown by all the twelve units examined, namely an initial steep increase in firing and then an increase along a much shallower slope. This

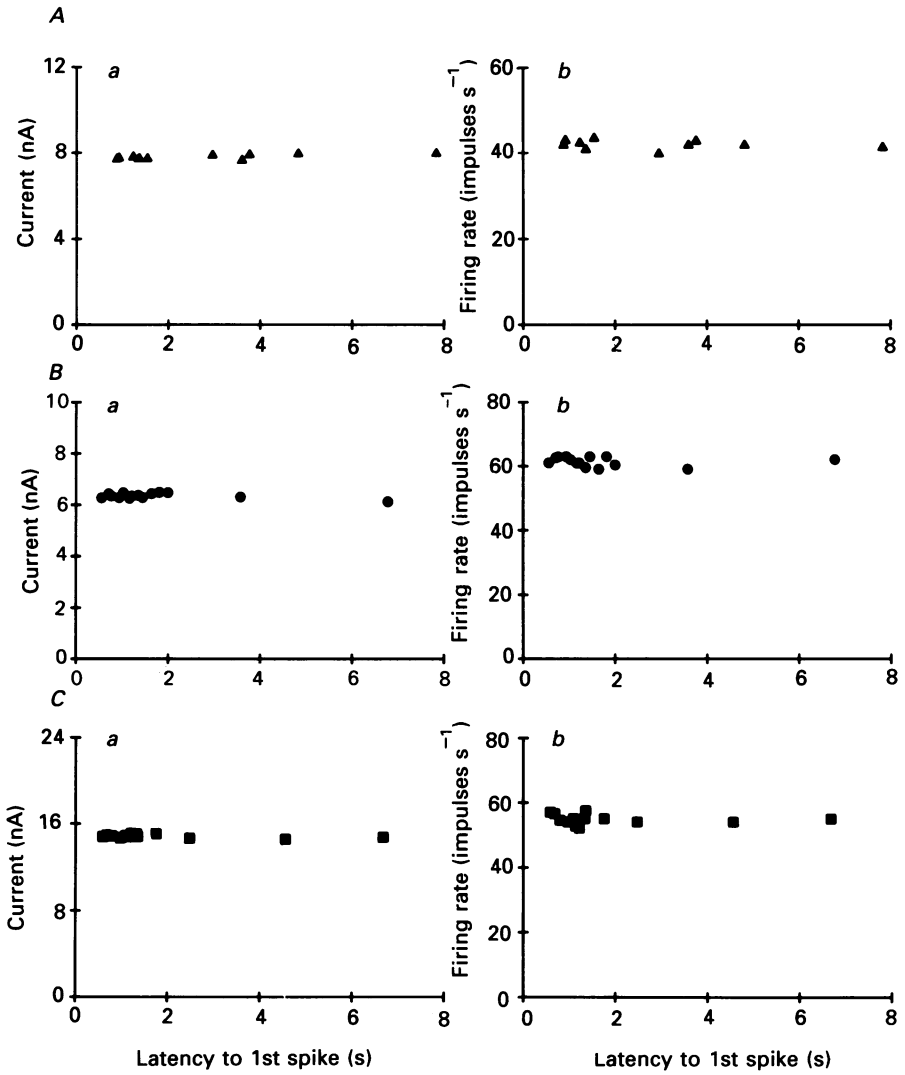

Fig. 9. Effects of changes in ramp velocity on threshold current needed to elicit firing (left-hand panels) and firing rate at the 'transition point' (right-hand panels) for three cells (*Aa* and *b*; *Ba* and *b*; *Ca* and *b*). The abscissa in all cases shows the latency from onset of ramp to firing of the first spike and so provides an indication of the ramp velocity because the shorter the latency the faster the ramp velocity. All data points shown are the average of five to ten repetitions of current at each frequency of the ramp. Note that both the threshold current for eliciting firing and firing at the transition point are both independent of ramp velocity. Neurone in *B* same as the one in Figs 8 and 7*D*.

pattern was common to all cells and a qualitative assessment indicated that it did not vary with changes in ramp velocity (Fig. 8). We were able to test this quantitatively in six cells in which we were able to systematically assess the effects of changing the ramp frequency on both the threshold for firing and the firing rate at the transition between the two slopes. The plots in Fig. 9 show that both parameters remain

constant with changes in ramp velocity. This suggests that over the frequency range studied the threshold for firing and firing frequency at the transition point are primarily governed by the amplitude of injected current and not by the rate of change of current.

DISCUSSION

We describe here the membrane and firing properties of a sample of elevator motoneurones and as such have provided the preliminary evidence needed for an assessment of their integrative properties. However, we have no formal evidence as to the functional types of motoneurones included in our sample and so must admit to some uncertainty as to the precise composition of our sample. Specifically we do not know the relative proportions of different functional subtypes of α-motoneurones, nor can we distinguish between α- and fusimotor motoneurones.

Fortunately the rat masseter muscle is composed almost entirely of type II muscle fibres (Schiaffino, 1974; Rowlerson, Mascarello, Barker & Saed, 1988), with type II A fibres being by far the most predominant type (Schiaffino, 1974; Rowlerson *et al.* 1988). Therefore the majority of the α-motoneurones in our sample would presumably innervate type II A muscle units and so would form an essentially homogenous population. This could in turn account for the failure to find relationships between the parameters plotted in Fig. 6 because the data from the hindlimb motoneurones indicate that there are no systematic variations in motoneurone electrical properties within a single functional subtype (Zengel *et al.* 1985). Mikhailov & Kuneev (rat: 1981) claimed to have identified α- and γ-motoneurones on the basis of differences in resting membrane potentials and antidromic latency. Presumed γ-motoneurones had membrane potentials of 40–60 mV and a mean antidromic latency of 0·24 ms whereas the corresponding values for α-motoneurones were 65–90 mV and 0·16 ms. The argument is unsatisfactory on two counts. First the latency difference could simply be a consequence of more pronounced damage inflicted at the soma by the electrode in the group with lower membrane potentials. This would slow conduction from the axon to soma and so increase antidromic latencies. Second the evidence in the cat is that conduction velocity alone cannot be used to separate α- and γ-motor fibres in the masseter nerve (Appenteng, Morimoto & Taylor, 1980). However, the possibility that some neurones both in their sample and ours were indeed γ-motoneurones is one that cannot be entirely dismissed if only because the criteria for doing so under the conditions of these experiments remain to be determined.

One factor that would affect the absolute values of the membrane properties reported would be the presence of an imperfect seal between the electrode and cell (Jack, 1979). This would introduce a leak conductance at the soma and the effect of such a passive conductance on R_n and τ_0 has been estimated by Gustafsson & Pinter (1984*a*) for a model neurone with an ideal membrane potential of -80 mV and a uniform value of R_m throughout its dendritic tree. Their analysis showed that at a membrane potential of -62 mV R_n would be underestimated by 30% and τ_0 by 16% (Gustafsson & Pinter, 1984*a*). The minimum membrane potential in our sample was -60 mV and so roughly similar errors would be expected in our estimates of R_n and

τ_0 on the assumption that the model is applicable to elevator motoneurones. The range of both R_n and τ_0 values in our sample was at least an order of magnitude greater than this (see Fig. 5) and so we would assume that the variation in these values primarily reflects genuine differences between neurones and is not simply the consequence of a variable leak conductance at the soma. We can therefore compare the results from elevator motoneurones to the much wider body of data available for cat hindlimb α-motoneurones with the aim of identifying similarities in organization.

Surprisingly both groups of motoneurones show a virtually identical range of R_n and τ_0 values. For example Gustafsson & Pinter (1984*a*) obtained a range of 0·6–4 MΩ for R_n (cf. 0·7–4·6 for elevators) and τ_0 values of 2–9 ms (cf. 1·5–9·6 ms). R_n is dependent on R_m and the geometry of the neurone ($R_n \propto R_m$/surface area). The mean soma diameters of elevator motoneurones are approximately half those of hindlimb motoneurones (rat, 15–35 μm; Rokx, van Willigen & Juch, 1985: cf. 30–70 μm for cat; Burke, Dum, Fleshamn, Glenn, Lev-Tov, O'Donovan & Pinter, 1982) and their surface areas also differ by a similar extent (Moore, 1988). Therefore the implication is that elevator motoneurones have a lower R_m than hindlimb motoneurones. A similar argument can be made for abducens motoneurones as these have much smaller surface areas than hindlimb motoneurones yet a similar range of R_n values (1·2 to 4·8 MΩ; Grantyn & Grantyn, 1978). Grantyn & Grantyn (1978) have suggested that there may be functional advantages in maintaining the same range of R_n across different populations of motoneurones. Increases in R_n introduce marked non-linearities in the summation of dendritic EPSPs and a more pronounced attenuation of their amplitude with distance from the soma (Rall & Rinzel, 1973; Rinzel & Rall, 1974). Therefore R_n may need to be constrained within quite a narrow range and this can be achieved by altering R_m or alternatively the complexity of branching in the dendritic tree. The relatively low R_n values of motoneurones (cf. 40·2 MΩ for hippocampal neurones; Brown, Fricke & Perkel, 1981) may be an adaptation to enhance the effective transfer of current along dendrites. By the same token non-linearities in current summation within the dendrites of hippocampal neurones may be an important factor controlling the behaviour of these neurones.

The firing characteristics of motoneurones are known to be closely correlated to the mechanical properties of the muscle units they innervate (for review see Kernell, 1983). There are no specific data on the twitch properties of individual motor units of elevator muscles but peak muscle tension is developed within 14 ms after the onset of direct electrical stimulation of the muscle and this then decays to half to its maximum amplitude in about the same time (Fig. 2; Nordstrom & Yemm, 1974). A similar experiment in the cat gave values of 13·1 ms for the time-to-peak tension and 12·8 ms to half-relaxation (Taylor, Cody & Bosley, 1973). This would suggest that the contractile characteristics of the masseter muscle are comparable to those of the abducens muscle for which times to peak tension for single motor units of 5–14 ms have been reported (cat: Goldberg, Lennerstrand & Hull, 1976). This compares with a mean time to peak tension of 27 ms for type FF motoneurones of the cat medial gastrocnemius motoneurones (Fleshman, Munson, Sypert & Friedman, 1981). Therefore elevator motoneurones would be expected to have properties similar to those of abducens motoneurones but faster than those of hindlimb motoneurones and this is borne out by a comparison of any aspect of the frequency–current relationship

of the cells. For example the maximum firing frequency within the primary range for hindlimb motoneurones (Kernell, 1965*a*) corresponds to the mean minimum frequency for the first interspike interval of elevator motoneurones and is close to the approximate mean of 45 impulses s^{-1} for abducens motoneurones (Figs 9–11 of Grantyn & Grantyn, 1978). Thus on these criteria the firing of elevator motoneurones would appear to accord broadly with expectations based on the behaviour of hindlimb motoneurones.

It can be argued that step increases in current intensity are a relatively unphysiological stimulus as the natural synaptic drive to motoneurones may occur over considerably slower time courses (see Bradley & Somjen, 1961). Jodkowski *et al.* (1988) have recently studied the response of phrenic motoneurones to slow current ramps (1 s duration). They reported that the threshold for firing remained constant with changes in ramp velocity and also that the subsequent firing was proportional to the intensity of injected current and independent of its frequency. In these respects there is complete agreement between the two sets of data and the dependence of firing on current intensity also agrees with the earlier report of Baldissera, Campadelli & Piccinelli (1984) that at frequencies below 1 Hz the peak firing rate of lumbosacral motoneurones to sinusoidal current waveforms was dependent on current intensity and not rate.

However Jodkowski *et al.* (1988) made no mention of firing increasing along two slopes in response to linearly rising ramps though this appears to be evident for one of the units shown by them (see Fig. 4*B*1 of Jodkowski *et al.* 1988). Therefore it is possible that other groups of motoneurones may fire in a similar manner as elevator motoneurones to ramp currents but this is clearly a point which needs to be examined. Our suggestion is that the initial steep slope in firing may be an adaptation to ensure that once activated motoneurone firing is rapidly brought up to a frequency at which contractions of the individual motor units would partially summate. The subsequent decrease in slope would then occur over the steep portion of the isometric frequency–tension curve of the motor unit. The result is that the gain for the motoneurone frequency–current relationship is the inverse of the motor unit frequency–force relationship. Firing at the transition point between the two slopes in our sample occurred at frequencies at which partially fused contractions are observed in the masseter muscle (Nordstrom & Yemm, 1974). It may be the case that firing at the transition point would vary for motoneurones innervating different muscle units and so provide a means of distinguishing different functional subtypes of motoneurones on the basis of their firing to slow ramp currents.

This work was supported by the MRC and the Wellcome Trust and formed part of the Ph.D. thesis of Jane Moore who was an MRC Scholar. It is a pleasure to acknowledge the excellent technical assistance of Lisa Conyers.

REFERENCES

APPENTENG, K., CONYERS, L. & MOORE, J. A. (1989). The monosynaptic excitatory connexions of single trigeminal interneurones to the V motor nucleus. *Journal of Physiology* **417**, 91–104.

APPENTENG, K., DONGA, R. & WILLIAMS, R. G. (1985). Morphological and electrophysiological determination of jaw-elevator muscle spindle afferents in rats. *Journal of Physiology* **369**, 93–113.

APPENTENG, K. & MOORE, J. A. (1986). Some membrane electrical properties of rat trigeminal motoneurones. *Journal of Physiology* **378**, 46*P*.

APPENTENG, K. & MOORE, J. A. (1987). Differences in the electrical properties of rat trigeminal motoneurones under two common anaesthetic regimes. *Journal of Physiology* **384**, 67*P*.

APPENTENG, K. & MOORE, J. A. (1988). The electrical geometry of rat trigeminal motoneurones. *Journal of Physiology* **396**, 55*P*.

APPENTENG, K., MORIMOTO, T. & TAYLOR, A. (1980). Fusimotor activity in masseter nerve of the cat during reflex jaw movements. *Journal of Physiology* **305**, 415–432.

BALDISSERA, F., CAMPADELLI, P. & PICCINELLI, L. (1984). The dynamic response of cat α motoneurones investigated by intracellular injection of sinusoidal currents. *Experimental Brain Research* **54**, 275–282.

BRADLEY, K. & SOMJEN, G. G. (1961). Accommodation in motoneurones of the rat and cat. *Journal of Physiology* **156**, 75–92.

BRAS, H., GOGAN, P. & TYC-DUMONT, S. (1987). The dendrites of single brainstem motoneurones intracellularly labelled with horseradish peroxidase in the cat. Morphological and electrophysiological differences. *Neuroscience* **22**, 947–970.

BROCK, L. G., COOMBS, J. S. & ECCLES, J. C. (1952). The recording of potentials from motoneurones with an intracellular electrode. *Journal of Physiology* **117**, 431–460.

BROWN, T. H., FRICKE, R. A. & PERKEL, D. H. (1981). Passive electrical constants in three classes of hippocampal neurons. *Journal of Neurophysiology* **46**, 812–827.

BURKE, R. E., DUM, R. P., FLESHMAN, J. W., GLENN, L. L., LEV-TOV, A., O'DONOVAN, M. J. & PINTER, M. J. (1982). An HRP study of the relation between cell size and motor unit type in cat ankle extensor motoneurons. *Journal of Comparative Neurology* **209**, 17–28.

BURKE, R. E. & TEN BRUGGENCATE, G. (1971). Electrotonic characteristics of alpha motoneurones of varying size. *Journal of Physiology* **212**, 1–20.

CLEMENTS, D. & REDMAN, S. J. (1989). Cable properties of cat spinal motoneurones measured by comparing voltage clamp, current clamp and intracellular staining. *Journal of Physiology* **409**, 63–87.

FLESHMAN, J. W., MUNSON, J. B., SYPERT, G. W. & FRIEDMAN, W. A. (1981). Rheobase, input resistance, and motor-unit type in medial gastrocnemius motoneurons in the cat. *Journal of Neurophysiology* **46**, 1326–1338.

FLESHMAN, J. W., SEGEV, I. & BURKE, R. E. (1988). Electrotonic architecture of type-identified α-motoneurones in the cat spinal cord. *Journal of Neurophysiology* **60**, 1–26.

GOLDBERG, S. J., LENNERSTRAND, G. & HULL, C. D. (1976). Motor unit responses in the lateral rectus muscle of the cat: intracellular current injection of abducens motoneurons. *Acta physiologica scandinavica* **96**, 58–63.

GRANIT, R., KERNELL, D. & SHORTESS, G. K. (1963*a*). Quantitative aspects of repetitive firing of mammalian motoneurones caused by injected currents. *Journal of Physiology* **168**, 911–931.

GRANIT, R., KERNELL, D. & SMITH, R. S. (1963*b*). Delayed depolarization and the repetitive response to intracellular stimulation of mammalian motoneurones. *Journal of Physiology* **168**, 890–910.

GRANTYN, R. & GRANTYN, A. (1978). Morphological and electrophysiological properties of cat abducens motoneurones. *Experimental Brain Research* **31**, 249–274.

GUSTAFFSON, B. & PINTER, M. J. (1984*a*). Relations among passive electrical properties of lumbar α-motoneurones of the cat. *Journal of Physiology* **356**, 401–431.

GUSTAFSSON, B. & PINTER, M. J. (1984*b*). An investigation of threshold properties among cat spinal α-motoneurones. *Journal of Physiology* **357**, 453–483.

ITO, M. & OSHIMA, T. (1965). Electrical behaviour of the motoneurone membrane during intracellularly applied current steps. *Journal of Physiology* **180**, 607–637.

JACK, J. J. B. (1979). An introduction to linear cable theory. In *The Neurosciences Fourth Study Program*, ed. SCHMITT, G. O. & WORDEN, F. G., pp. 324–357. MIT Press, Cambridge, MA, USA.

JODKOWSKI, J. S., VIANA, F., DICK, T. E. & BERGER, A. J. (1987). Electrical properties of phrenic motoneurons in the cat: Correlation with inspiratory drive. *Journal of Neurophysiology* **58**, 105–124.

JODKOWSKI, J. S., VIANA, F., DICK, T. E. & BERGER, A. J. (1988). Repetitive firing properties of phrenic motoneurones in the cat. *Journal of Neurophysiology* **60**, 687–702.

KERNELL, D. (1965*a*). High frequency repetitive firing of cat lumbosacral motoneurones stimulated by long lasting injected currents. *Acta physiologica scandinavica* **65**, 74–86.

KERNELL, D. (1965*b*). The limits of firing frequency in cat lumbosacral motoneurones possessing different time course of afterhyperpolariztion. *Acta physiologica scandinavica* **65**, 87–100.

KERNELL, D. (1979). Rhythmic properties of motoneurones innervating muscle fibres of different speed in m. gastrocnemius medialis of the cat. *Brain Research* **160**, 159–162.

KERNELL, D. (1983). Functional properties of spinal motoneurons and gradation of muscle force. In *Motor Control Mechanisms in Health and Disease*, ed. DESMEDT, J. E., pp. 213–226. Raven Press, New York.

MIKHAILOV, V. V. & KUNEEV, N. V. (1981). Membrane electrical properties of motoneurones innervating the masseter muscles in rat. *Neurophysiology* **13**, 195–199.

MOORE, J. A. (1988). The electrical geometry and passive membrane properties of rat jaw-elevator motoneurones. Ph.D. Thesis, University of Leeds.

MOORE, J. A. & APPENTENG, K. (1989). The morphology of the axons and axon collaterals of rat jaw-elevator motoneurones. *Brain Research* **489**, 383–386.

NORDSTROM, S. H. & YEMM, R. (1974). The relationship between jaw position and isometric active tension produced by direct stimulation of the rat masseter muscle. *Archives of Oral Biology* **19**, 353–359.

RALL, W. (1959). Branching dendritic trees and motoneuron membrane resistivity. *Experimental Neurology* **1**, 491–527.

RALL, W. (1977). Core conductor theory and cable properties of neurons. In *Handbook of Physiology, The Nervous System*, ed. BROOKHART, J. M. & MOUNTCASTLE, V. B., pp. 39–97. American Physiological Society, Bethesda, MD, USA.

RALL, W. & RINZEL, J. (1973). Branch input resistance and steady attenuation for input to one branch of a dendritic neuron model. *Biophysical Journal* **13**, 648–688.

RINZEL, J. & RALL, W. (1974). Transient response in a dendritic neuron model for current injected at one branch. *Biophysical Journal* **14**, 759–790.

ROKX, J. T. M., VAN WILLIGEN, J. D. & JUCH, P. J. W. (1985). Distribution of innervating neurons of masticatory muscle spindles in the rat, an HRP study. *Experimental Neurology* **88**, 562–570.

ROSE, P. K. & VANNER, S. J. (1988). Differences in the somatic and dendritic specific membrane resistivity of spinal motoneurones – an electrophysiological study of neck and shoulder motoneurons in the cat. *Journal of Neurophysiology* **60**, 148–174.

ROWLERSON, A., MASCARELLO, F., BARKER, D. & SAED, H. (1988). Muscle-spindle distribution in relation to the fibre-type composition of masseter in mammals. *Journal of Anatomy* **161**, 37–60.

SCHIAFFINO, S. (1974). Histochemical enzyme profile in the masseter muscle in different mammalian species. *Anatomical Records* **18**, 53–62.

TAKATA, M., FUJITA, S. & KANAMORI, N. (1982). Repetitive firing in trigeminal mesencephalic tract neurons and trigeminal motoneurons. *Journal of Neurophysiology* **47**, 23–30.

TAYLOR, A., CODY, W. J. & BOSLEY, M. A. (1973). Histochemical and mechanical properties of the jaw muscles of the cat. *Experimental Neurology* **38**, 99–109.

VORNOV, J. J. & SUTIN, A. J. (1986). Noradrenergic hyperinnervation of the motor trigeminal nucleus: Alterations in membrane properties and response to synaptic input. *Journal of Neuroscience* **6**, 30–37.

ZENGEL, J. E., REID, S. A., SYPERT, G. W. & MUNSON, J. B. (1985). Membrane electrical properties and prediction of motor-unit type of medial gastrocnemius in the cat. *Journal of Neurophysiology* **53**, 1323–1344.